KOHN, BARRY H.

LASER INDUCED CHEMICAL FLUORESCENCE STUDIES

City University of New York PH.D. 1981

LASER INDUCED CHEMICAL FLUORESCENCE STUDIES

by

Barry H. Kohn

A dissertation submitted to the Graduate Faculty in Chemistry in partial fulfillment of the requirements for the degree of Doctor of Philosophy, The City University of New York

1981

This manuscript has been read and accepted for the Graduate Faculty in Chemistry in satisfaction of the dissertation requirement for the degree of Doctor of Philosophy.

12/12/80
date

A. M. [signature]
Chairman of Examining Committee

12 December 1980
date

David C. Locke
Executive Officer

A. M. [signature]

[signature]

[signature]

Supervisory Committee

The City University of New York

ABSTRACT

Laser Induced Chemical Fluorescence

by

Barry H. Kohn

Advisor: Professor A. M. Ronn

The activation and deactivation rate constants for deuterated methyl fluoride and methyl chloride have been determined. For CD_3F activation of the ν_1, ν_4 state occurs with a rate constant of 680 $msec^{-1}$ $torr^{-1}$; for CD_3Cl the ν_1 state is populated with a rate constant of 490 $msec^{-1}$ $torr^{-1}$ and the ν_3 state, 52 $msec^{-1}$ $torr^{-1}$. Self deactivation of CD_3F occurs with a rate constant of 0.44 $msec^{-1}$ $torr^{-1}$ while for CD_3Cl this process exhibits double exponential behavior resolving to 51 $msec^{-1}$ $torr^{-1}$ and 2.8 $msec^{-1}$ $torr^{-1}$. The data is discussed in light of existing theoretical models.

DEDICATION

To my parents

To my sister

and

To my dear wife, Judy, for her continuing patience, support, and encouragement.

ACKNOWLEDGMENT

I wish to express my sincerest gratitude to my mentor, Professor Avigdor M. Ronn for the guidance and encouragement he has provided over these years and most importantly for his continued friendship. I am most grateful to Dr. Leonard Gamss for his assistance, co-operation, and numerous friendly and enlightening discussions. To Dr. Boyd Earl, Dr. Shu Lee and Dr. Y. Langsam, thanks for many stimulating conversations. Of course, my appreciation to the entire faculty and staff of City University of New York for their co-operation.

TABLE OF CONTENTS

FIGURES AND TABLES

FIGURES

TABLES

Chapter 1 - General Introduction

The mechanisms of intra molecular transfer of energy among the vibrational, rotational and translational degrees of freedom has long been of interest to scientists. The development of the laser with its potential for driving isotopically selective reactions has lent greater import to the complete understanding of these energy transfer modes. Chemical reactions, which by their very nature involve the creating and breaking of chemical bonds, are intimately affected by the energy of those bonds and the relative motion of the atoms with respect to them. These factors, as expressed in the vibrational modes of the molecules and interactions with the other degrees of freedom, are thus of critical importance in the study of chemistry.

Prior to the development of the laser, researchers relied on the use of excitation devices such as flashlamps, shock tubes and ultrasonic generators to create non-equilibrium populations in one or more of the energy modes of the molecule.(1) The relaxation of these populations could then be followed and information extracted about the energy transfer processes involved. However, these processes suffer from relative non-specificity as to

the exact energy level or mode excited. The availability of a monochromatic, high intensity laser has made possible, for the first time, the excitation of particular vibrational energy states of individual molecules. Pulsed infrared (IR) lasers can be used to instantaneously create large populations of excited molecules. These molecules are excited to a specific vibrational energy level, while the rest of the vibrational manifold and all other degrees of freedom remain unperturbed.

This technique has given rise to the field of laser induced fluorescence. Following laser excitation of a particular vibrational energy level of one of the gases, the infrared fluorescence of a molecular gas or gas mixture is monitored as a function of wavelength and time. These kinds of studies yield information about the collisional energy transfer processes which occur among the molecules in question. In polyatomic gases excited by IR radiation two such processes are of interest. These correspond to transfer of the laser supplied excess energy, either to vibrational levels other than the pumped level (V-V) or into translational or rotational energy (V-T/R). The rates of these processes

are measured as a function of pressure of the collision partners and the rate constants deduced.

The most important precondition of the use of this method is the wavelength matching of a laser line with a suitable transition in a molecule. Due to the ever increasing numbers of IR lasers available, this requirement is less severe than it may seem. Furthermore, even this condition has been circumvented by the use of indirect molecular pumping.[2]

In Chapters 2 and 3 the application of this method to the study of energy transfer in deuterated methyl fluoride (CD_3F) and deuterated methyl chloride (CD_3Cl) is presented. Rate constants are reported for the V-V processes involved and for the V-T/R deactivations with the rare gases and with self as collision partners. An interpretation of the relative magnitude of the observed rates is presented based on existing V-T/R theory and on a consideration of the energy level scheme for the molecule. A brief preliminary report of these results has been given earlier[3, 4] followed by a more detailed presentation.[5, 6]

Chapter 2 - CD_3F Studies

Experimental

The basic experiment consists of utilizing an IR photo detector to monitor the fluorescences from a sample of gas following excitation by a Q switch CO_2 laser whose energy output corresponds to the pumped vibrational mode of the compound being studied.

A schemetic diagram of the experimental apparatus is presented in Figure 1. The excitation source was a Q switch CO_2-N_2 - He laser. Population inversion in CO_2 and consequent lasing is achieved by continuously sustaining a high voltage (25 kV) discharge in a two meter tube in which a mixture of CO_2: N_2: He, at a ratio of 1:2:8 and total pressure of 20 torr is flowed. The cavity of the laser is terminated at one end by a 100% reflecting mirror mounted on a rotating frame whose rotation frequency is controlled by an amplifier oscillator system. The rotation frequency was variable between 50 and 400 Hz but was usually left fixed at 94 Hz. This was found to be the optimum rate since it represented a compromise between decreasing laser output power with higher repetition rates and the longer averaging time needed to obtain measurable signals at lower repetition rates.

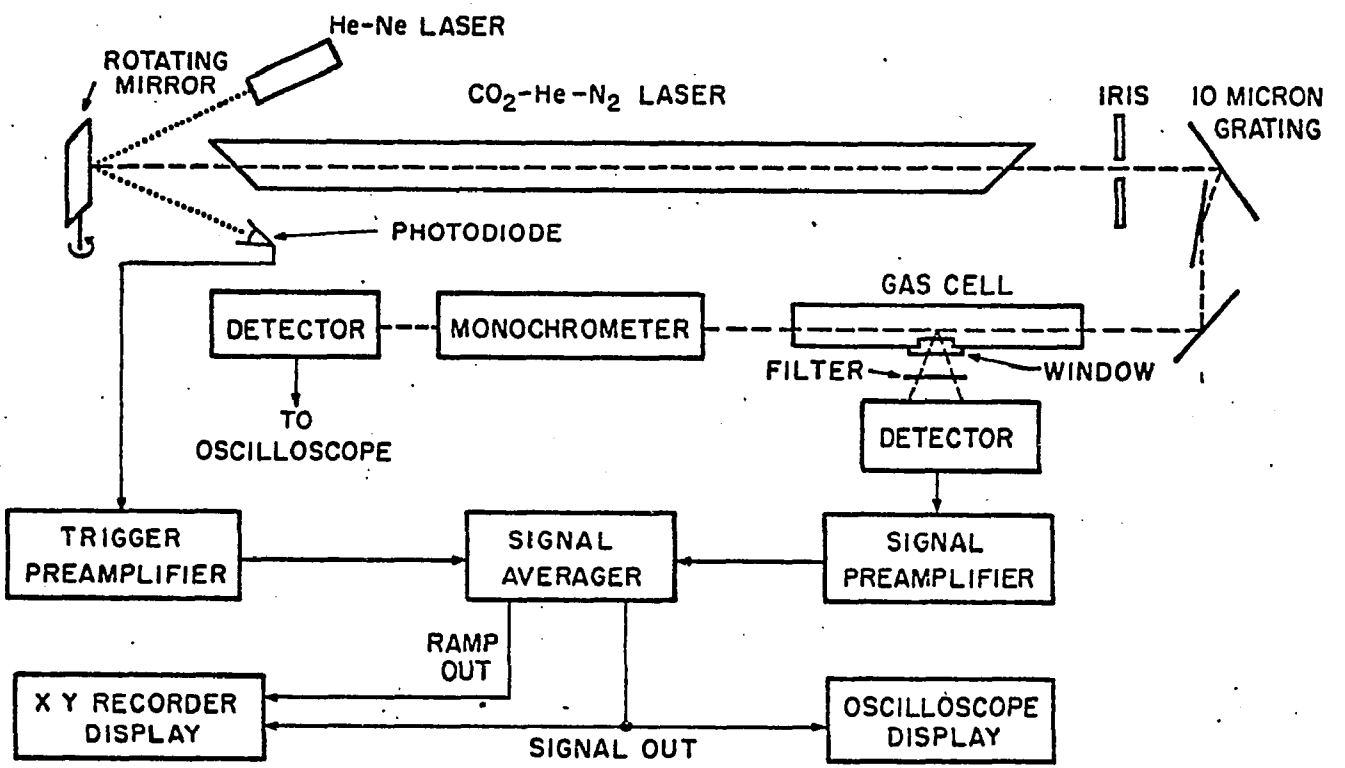

Figure 1. Schematic diagram of apparatus utilized for energy transfer studies

The other end is terminated by a diffraction grating blazed for 10μ (75 lines/inch) mounted in the Littrow configuration. With this arrangement, the grating provides feedback on its 1st order and outcouples on the 0th order. Grating rotation provides for frequency selection across two vibration-rotation bands of CO_2 (i.e., 001-01^{o}0 at 10.6μ and 001-02^{o}0 at 9.6μ.). A typical laser output was a one millijoule pulse with a width of 400 nsec at half maximum.

The laser beam was passed through a gas sample cell via sodium chloride windows and was monitored with a monochromator and a high speed infrared detector (Au:Ge). The detector output was continuously displayed on an oscilloscope. Fluorescence was observed through a third window at right angles to the laser beam axis. The window material was chosen so as to pass the expected fluorescence wavelengths while blocking the scattered laser light. In addition IR interference filters were placed between that window and the IR detector which was used to monitor the fluorescence as so to further isolate the signal of interest.

For study of 4-5μ emissions of CD_3F and CD_3Cl

a MgF_2 window was selected and used in combination with a liquid nitrogen cooled InSb photovoltaic detector. Study of the ν_3 level of CD_3Cl necessitated the use of a system capable of detecting longer wavelengths i.e. 14μ. For this purpose a liquid helium cooled Cu:Ge photo conductive detector was selected and the emission was passed through a KBr window. To suppress scattered laser radiation, two IR interference filters (a 13μ longpass and a 14-22μ bandpass filter) were used.

In all cases the output signals from the detector were amplified and then passed to a P.A.R. THD-9 Waveform Eductor where they were accumulated and averaged. The eductor output was then displayed on an oscilloscope and a permanent record made on an x-y recorder. All the electronics were pre-triggered by a He-Ne laser-photodiode combination which allowed for an adjustable time delay between the triggering of the eductor and the onset of laser oscillation. In this way a true baseline for the fluorescence signal could be determined. Electronic response times for the entire system were 1.5μs for the InSb detector and 4μs for the Cu:Ge detector.

The studies were carried out on CD_3F obtained

from Merck and Company Incorporated of St. Louis, Missouri, specified as having 99.5% isotopic and 99% molecular purities; the most probable contaminants being organic substances used in the synthesis. Further purification by adsorption on anhydrous $Ba(OH)_2$ was carried out in the laboratory to remove any trace of carbon dioxide and water. The CD_3Cl used was obtained from Merck and Company Incorporated of Rahway, New Jersey, specified as having 99.5% isotopic and 99% molecular purities.

The rare gases, except for ^3He, were Matheson research grade with impurities of greater than 1 ppm listed as ^4He ($Ne<5$); Ne ($He<10$, $H_2<4$, $Ar<5$); $Ar(N_2<5)$, Kr ($Xe<25$, $N_2<25$, $O_2<4$, $H_2<5$, hydrocarbons<10); Xe ($Kr<50$, $N_2<10$, $O_2<5$, $Ar<5$, $H_2<10$ hydrocarbons<10). The ^3He was obtained from Mound Laboratories and was specified as having 99.5% isotopic and 99.9% atomic purities.

Gas pressures were measured with an MKS Baratron capacitance manometer attached directly to the all glass sample cell. A second port on the cell was attached directly to the gas handling system which consisted of a glass and stainless steel vacuum system with an oil diffusion pump backed by a mechanical pump.

Activation and deactivation measurements on the pure samples were made by adding incremental amounts of CD_3X (i.e. either CD_3F or CD_3Cl) to the cell. For the CD_3X-rare gas deactivation measurements, incremental amounts of the rare gases were added to a fixed amount of CD_3X already in the cell. Whenever necessary a fixed, but sufficient, amount of Xe was added as a buffer gas to suppress the heating that resulted from the degradation of the laser energy. Before measurements were initiated, sufficient time (typically five to ten minutes) was allowed for complete mixing of all gases present. Typical outgas rates for the cell and gas manifold were less than 5 millitorr/hour.

Analysis of the data was accomplished by semi-log plotting the fluorescence intensity vs. time to obtain the deactivation rates for a set of pressures. A least squares fit of deactivation rate vs. pressure produced a curve whose slope corresponds to the rate constant for the process studied.

Results

Upon irradiation of a sample of CD_3F with the R (24) vibrational-rotational line of a Q switch 10.6μ CO_2 laser, (with a frequency of a 978 cm^{-1} (1)) a strong fluorescence signal was observed in the 4-5μ spectral region. As can be noted from the partial energy level diagram (Figure 2) and the table of spectral data (Table 1) this corresponds to pumping the $0 \rightarrow \nu_3$ vibrational transition and fluorescence from the ν_1 and ν_4 levels.

Fluorescence from these two levels was also observed subsequent to pumping of the ν_5 and ν_6 states of CD_3F with the appropriate laser lines. However these latter signals were of a relatively lower intensity. Because of the fast V-V equilibration between the states, it was decided that no new information could be obtained from further study of vibrational energy transfer which results from pumping the $0 \rightarrow \nu_5$ and $0 \rightarrow \nu_6$ transitions.

The fluorescence signal in the 4-5μ region was the only one observed and studied. The reason for this is revealed upon examination of Figure 2. The grouping of vibrational fundamentals around the 1000 cm^{-1} and 2000 cm^{-1} regions precludes observation of fluorescence emissions other than 4-5μ

TABLE 1

Spectral data for CD_3F (2)

Symmetry Species	No.	Approximate Type of Mode[1,2]	Absorption Frequency (cm^{-1})
a_1	ν_1	CD_3 s-stretch	2110
a_1	ν_2	CD_3 s-deform	1136
a_1	ν_3	CF stretch	991
e	ν_4	CD_3 d-stretch	2258
e	ν_5	CD_3 d-deform	1072
e	ν_6	CD_3 rock	903

1. s = symmetric

2. d = degenerate

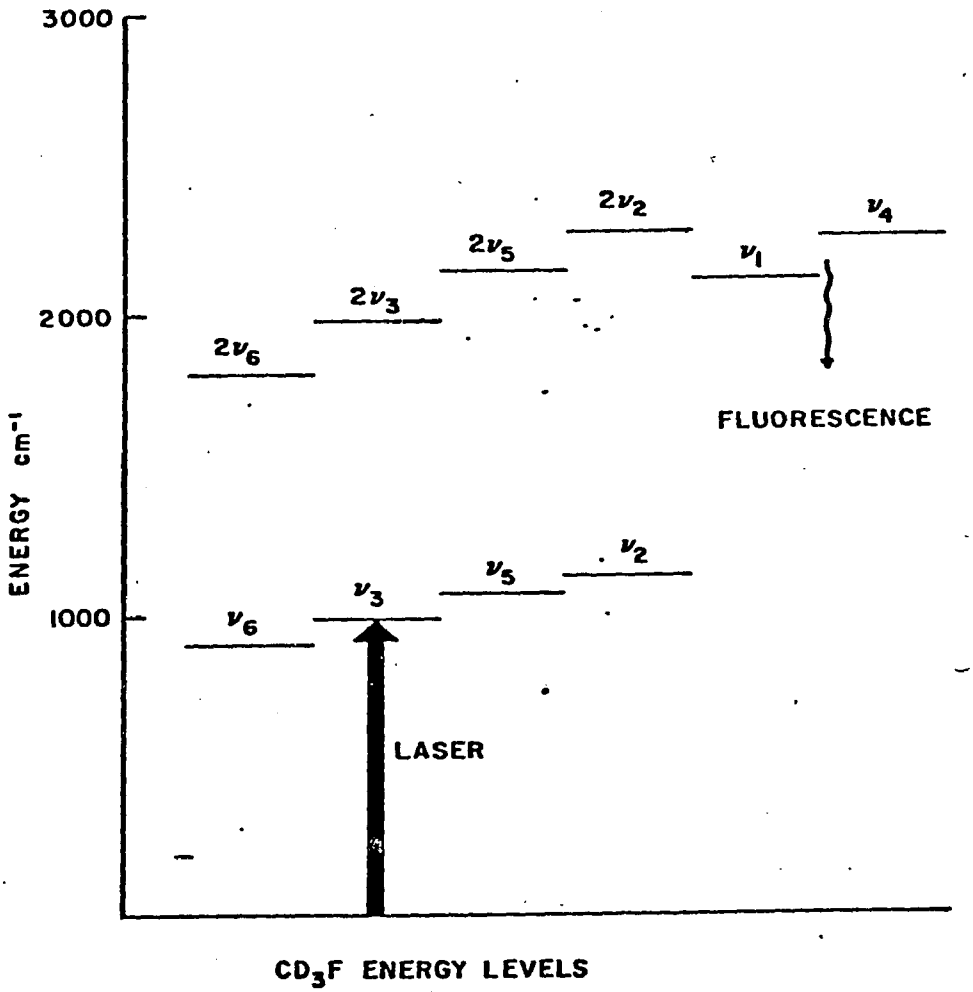

Figure 2. Partial energy level diagram for CD_3F

originating from the upper levels. Signals from the lower set of levels at approximately 10μ are ruled out due to the large component of laser scatter at that wavelength. Signals from the first overtones or combination bands of the lower fundamentals will again fall into the 4-5μ region. Since these signals consist of considerably lower intensity, they will only marginally add to the strong ν_1, and medium ν_4 emissions.

Fluorescence from the 3000 cm^{-1} region, corresponding to emission from the second overtones of the lower set and/or combination bands of the lower and upper fundamentals, was also not observed. This did not occur despite the existence of efficient collisional pumping mechanisms for populating these states [3] and despite the fact that the InSb detector is quite capable of seeing 3μ signals. Again, this is almost certainly due to the relatively low emission intensity of these states. Thus, access to the vibrational energy transfer of CD_3F is limited to the 4-5μ window. This is in contrast to other molecules studied by laser induced fluorescence in which as many as four different fluorescence signals were observed.[4]

The V-T/R deactivation rate constants for CD_3F-CD_3F collisions as well as CD_3F-rare gas collisions were measured, and the results are presented in Table 2. A typical plot of deactivation rate vs. pressure of collision partner (in this case for ^4He) is presented in Figure 3.

The activation rate constant of the ν_1, ν_4 levels was measured by analysis of the rise time of the 4-5 fluorescence at low pressure ($<$ 1 torr) of CD_3F. A value of 680 $msec^{-1}$ $torr^{-1}$ was obtained.

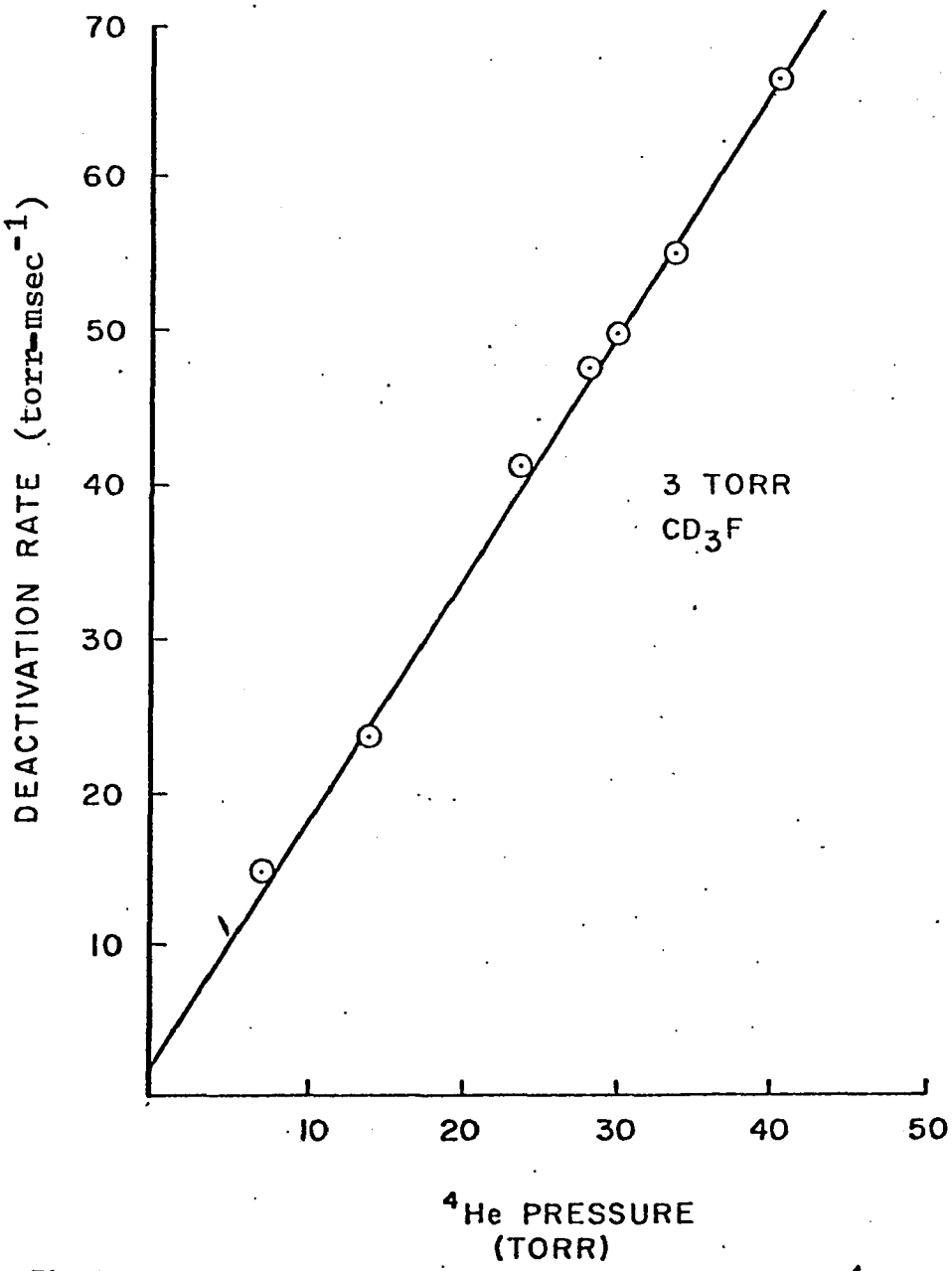

Figure 3. Plot of deactivation rates as a function of ^{4}He pressure (with a fixed CD_3F pressure of 3torr).
Slope=1.57 $ms^{-1}torr^{-1}$

TABLE 2

DEACTIVATION RATE CONSTANTS AND PROBABILITIES

Collision Partner	μ_{CD_3F-X} (amu)	$\mu^{1/2}$	σ (Å) [a]	Rate constant $msec^{-1}torr^{-1}$ [b]	Z [c]	$P_{exp} \times 10^3$ [d]	$P_{theor} \times 10^3$ [e]
^3He	2.79	1.67	2.58	3.26	4600	0.217	9.84
^4He	3.61	1.90	2.58	1.57	8300	0.120	6.15
Ne	12.96	3.61	2.86	0.12	65300	0.0153	0.139
Ar	19.18	4.38	3.47	0.074	101500	0.00990	0.0288
Kr	25.70	5.07	3.61	0.025	221800	0.00451	0.00654
Xe	28.84	5.37	4.06	0.082	86400	0.0120	0.00340
CD_3F	18.49	4.30	3.65	0.44	18000	0.0555	0.0408

(a) J. O. Hirschfelder, C. F. Curtis and R. B. Bird, Molecular Theory of Gases and Liquids (Wiley, New York, 1954)

(b) Error limits are ±10% of reported values.

(c) Number of collisions needed for deactivation, rounded off to nearest hundreds place.

$$Z = 2.56 \times 10^6 \left(\frac{\sigma_a + \sigma_b}{2}\right)^2 \mu^{-1/2} \left(10^{-3}/\text{rate}\right)$$

(d) Experimental probability/collision. $P_{exp} = 1/Z$

(e) Theoretical probability of deactivation through ν_6, calculated using SSH theory and including the breathing sphere parameter $\langle A_6^2 \rangle = .0963$.

Discussion

Before discussing the results of this experiment, a brief overview of energy transfer processes is appropriate.

Upon laser irradiation, a certain fraction of the sample gas is excited to some vibrational state ν_i which corresponds to the pumped mode for the molecule. From this condition there are two broad classes of energy transfer available to the system in its progression back to an equilibrium state. These are vibration to vibration (V-V) and vibration to translation/rotation (V-T/R).

It is useful to further subdivide V-V processes into two subtypes: intramodal and intermodal events. Intramodal events tend to populate overtones via collision of two excited molecules:

$$CH_3\ X\ (\nu_i) + CH_3\ X\ (\nu_i) \rightleftharpoons CH_3\ X\ (2\nu_i) + CH_3\ X\ (0) + \Delta E\ (\text{small}) \qquad (1)$$

Such "up the ladder" processes within a single manifold, being nearly resonant, are expected to be very efficient. Experimental measurements of these types of processes have yielded cross sections of approximately one-fifth to one-third the gas kinetic value.[3, 5, 6] Similar behavior would be expected in

populating combination bands by collisions of molecules in two different excited states. Such processes include:

$$CH_3\ X\ (\nu_i) + CH_3\ X\ (\nu_j) \rightleftharpoons CH_3\ X\ (\nu_i + \nu_j) + CH_3\ X\ (0) + \Delta E\ (\text{small}) \quad (2)$$

Such an event would also be nearly resonant and could be considered to be of the "intra manifold type."

In contrast one may consider a process in which one member of the colliding pair is initially in the ground state, the collision of which results in a molecule in a different excited state

$$CH_3\ X\ (n\nu_i) + CH_3\ X\ (0)\ (\text{or M}) + \Delta E \rightleftharpoons CH_3\ X\ (m\nu_j) + CH_3\ X\ (0)\ (\text{or M}) \quad (3)$$

The resulting energy deficit, ΔE, of such an intermodal process may be quite large and is determined by the energy levels of the states involved. These intermodal processes will distribute the excess vibrational energy among all the normal modes following the initial mode-specific excitation. It should be noted that the collision partner may be a molecule of a different species such as a rare gas atom (M).

In V-T/R transfer an excited molecule collides

with another molecule; the excess vibrational energy is converted into translational and rotational energy

$$CH_3X(\nu_i) + CH_3X \text{ (or M)} \rightleftharpoons CH_3X(0) + CH_3X \text{ (or M)} + \Delta E \quad (4)$$

The energy excess resulting from such a process is simply equal to the energy of the state which is deactivated, typically several hundred wave numbers. The collision partner may be in any state. In addition, it may consist of a different species.

While such processes are normally referred to as V-T/R, it should be noted that there will be a V-T/R component to any energy transfer process which is not perfectly resonant. Thus, any energy defect in a V-V process will be precisely compensated for by changes in translation and rotation in order to satisfy the demands of energy conservation.

Following complete V-T/R relaxation the translational energy content of the sample is clearly in excess of the pre-excitational value. The final step in the overall relaxation process is the thermal equilibration of the sample with the environment. This process occurs by diffusional transport to the cell walls. In the pressure regimes used in these experiments, this process occurs over a period of

milliseconds (a time scale much longer than any of interest in the vibrational relaxation).

The classification of energy transfer processes into these three subclasses is important because by classifying an energy transfer event in this fashion, one can appreciate the energy defect involved. It is this factor, more than any other single parameter, which determines the efficiency of a collisional energy transfer process. A theory of such processes, in which the repulsive part of the intermolecular potential dominates the hard collision regime, was developed by Schwartz, Slawsky and Herzfeld (SSH) [7, 8] and later modified by Stretton [9] and Tanczos [10]. In this theory, the probability per gas kinetic collision that an energy transfer event will occur is proportional to the product of an integral over the available collision energies, which brings in the energy defect information, and the breathing sphere parameter $\langle A_i^2 \rangle$ for the normal modes involved.

In agreement with the above discourse, almost all laser induced fluorescence studies done to date have yielded a vibrational energy transfer scheme which is characterized by very efficient V-V processes

and a slower V-T/R deactivation (3); thus, there is rapid equilibration of the laser pumped level and all of the other excited energy levels followed by a uniform relaxation of the entire system to the ground state. In CD_3F, this model is particularly applicable and most easily understandable because of the way the energy levels are spaced. The lowest four fundamentals are centered around the pumped ν_3 state and are separated by a maximum of 233 cm^{-1}. This allows for a very rapid dispersal of the excess laser energy by such processes as:

$$CD_3F(\nu_3) + CD_3F(0) \rightleftharpoons CD_3F(\nu_6) + CD_3F(0) + 88\ cm^{-1} \quad (5)$$

$$CD_3F(\nu_3) + CD_3F(0) \rightleftharpoons CD_3F(\nu_5) + CD_3F(0) - 81\ cm^{-1} \quad (6)$$

$$CD_3F(\nu_3) + CD_3F(0) \rightleftharpoons CD_3F(\nu_2) + CD_3F(0) - 145\ cm^{-1} \quad (7)$$

The relatively small amounts of energy given up to, or taken out of the translational and rotational degrees of freedom, which are involved in these engery transfers, ensure their efficiency.

The excitation is simultaneously communicated to the 2000 cm^{-1} region by the near resonant equilibration of these fundamentals and their first overtones, by the general process

$$CD_3F(\nu_i) + CD_3F(\nu_i) \rightleftharpoons CD_3F(2\nu_i) + CD_3F(0) + \approx 0 \text{ cm}^{-1} \quad (8)$$

where i = 2, 3, 5, 6.

From the overtones it is just a short step over to the fluorescing ν_1 and ν_4 states by such transfer expressions as

$$CD_3F(2\nu_5) + CD_3F(0) \rightleftharpoons CD_3F(\nu_1) + CD_3F(0) + \Delta E \quad (9)$$

where $\Delta E \approx 34 \text{ cm}^{-1}$

and

$$CD_3F(2\nu_2) + CD_3F(0) \rightleftharpoons CD_3F(\nu_4) + CD_3F(0) + \Delta E \quad (10)$$

where $\Delta E \approx 14 \text{ cm}^{-1}$

where equation (9) is a particularly fast process because of Fermi resonance between the $2\nu_5$ and ν_1 levels. (11)

Thus the energy deposited in the ν_3 level by the laser pulse is very quickly distributed among the nearby fundamentals and then transferred to the ν_1 and the ν_4 levels (probably by crossover from the overtones). Alternately, the excitation can reach the latter levels by more direct routes such as

$$CD_3F(\nu_3) + CD_3F(\nu_2) \rightleftharpoons CD_3F(\nu_1) + CD_3F(0) + 17 \text{ cm}^{-1} \quad (11)$$

and

$$CD_3F(\nu_5) + CD_3F(\nu_2) \rightleftharpoons CD_3F(\nu_4) + CD_3F(0) \quad (12)$$
$$-50\ cm^{-1}$$

Though more direct, such collisional energy transfer events require the simultaneous change of two vibrational quanta on one molecule and one on the other. Such events are expected to be less efficient than processes requiring only one quantum change for each molecule. Exceptions to this rule, which results from simple arguments based on the Born approximation, can occur. This is particularly true for collision events such as eq. (9) where significant Fermi mixing of an overtone and a fundamental arises. This does not appear to be the case for processes (11) and (12) though they cannot be ruled out with absolute certainty at this time. In any event, the energy deficits are such that a rapid V-V activation of the ν_1, ν_4 states would be expected, and the value of 680 $msec^{-1}$ $torr^{-1}$ observed for the fluorescence rate constant is consistent with results obtained for other members of the deuterated methyl halide series where analagous pathways are available[12-14]. In contrast members of the nondeuterated methyl halide series exhibit ν_1, ν_4 activation rate constants in the range of 100 - 200

$msec^{-1}$ $torr^{-1}$. It should be noted that activation of the ν_1, ν_4 state of the nondeuterated series cannot proceed directly from the first overtones, requiring the third harmonic as an intermediary[15-18].

The V-T/R deactivation rate constants presented in Table 2 are in general qualitative agreement with the results for similar molecules and particularly with those of the nondeuterated species CH_3F[19-20]. The CD_3F self deactivation rate constant, 0.44 $msec^{-1}$ $torr^{-1}$ is the same order of magnitude as the 0.59 $msec^{-1}$ $torr^{-1}$ reported for CH_3F. The CD_3F rare gas rate constants also behave as expected; decreasing with increasing mass of the collision partner except for an unexplained higher value for Xe. Again, with the exception of the Xe case the general trend of these results and their magnitudes are similar to those observed for CH_3F. A more informative method of interpreting the V-T/R relaxation results consists of examining the probability of deactivation as a function of the reduced mass of the collision partners. This is shown in Figure 4 where both the theoretical and experimental results are presented.

The theoretical curve calculated by the SSH

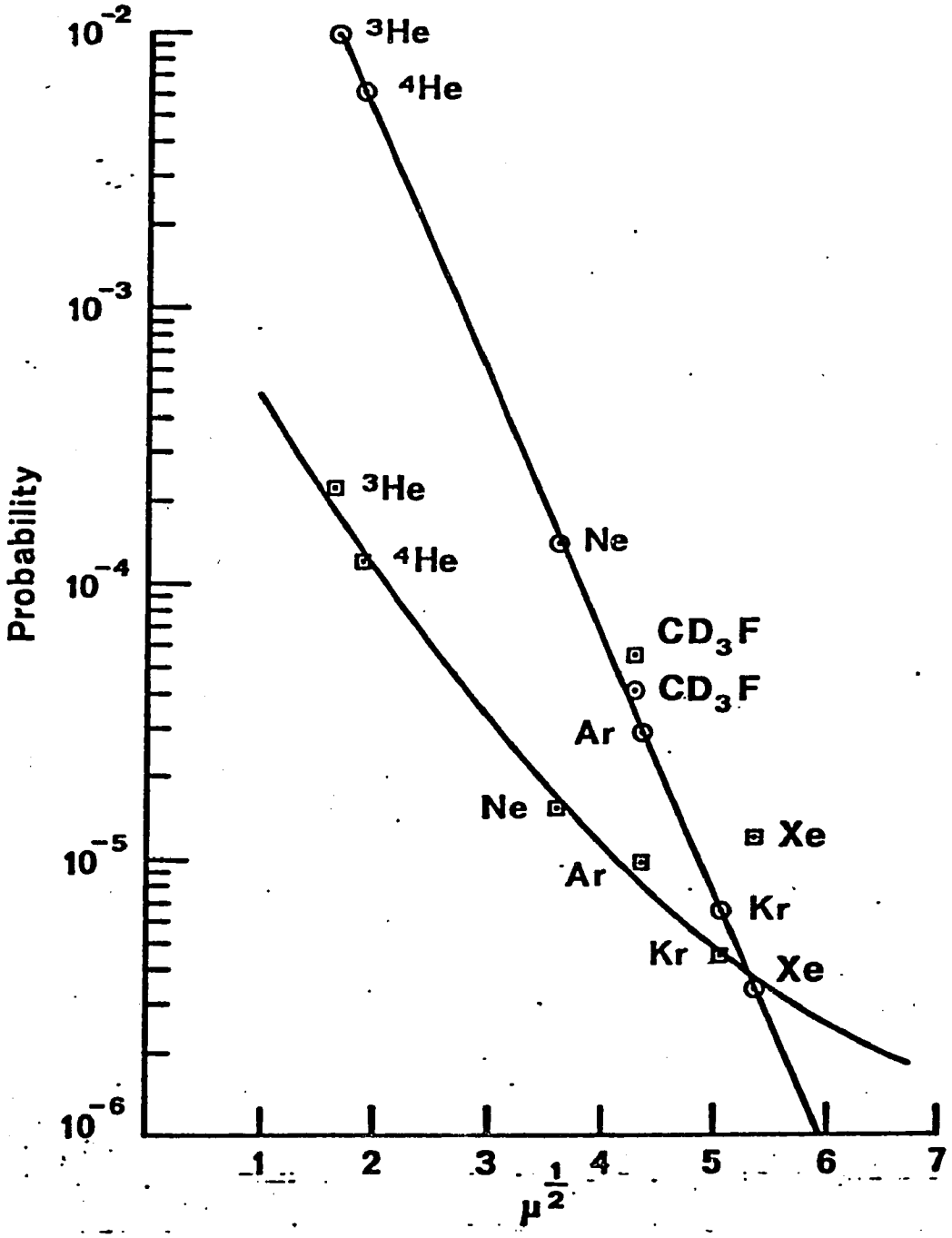

Figure 4. Plot of experimental(⊡) and theoretical(⊙) probabilities as a function of the square root of the reduced mass of the collision partners

type V-T theory, as modified by Stretton to include breathing sphere parameters, yields a straight line which predicts decreasing relative probability as the rare gas is varied from ^{3}He to Xe. This is a direct result of the SSH model which allows for the excess vibrational energy to be taken up only by the translational degrees of freedom. Thus, the deactivation probability is intimately related to the relative translational velocity of the colliding molecules which decreases with the increasing mass of the rare gas. The experimental curve of Figure 4, which is based on a ratio of the observed relaxation rate constants to the gas kinetic, seems to diverge from a straight line. This disagreement with the theoretical V-T behavior can be explained if the rotational degrees of freedom are also allowed to take up the excess energy by vibration-rotation (V-R) energy transfer. According to Moore[21], V-R processes become important compared to V-T processes when the rotational velocity of the collision system is greater than the translational velocity. This condition is more easily satisfied by the heavier rare gases and leads to the decreasing slope of the experimental curve of Figure 4. Indeed, this leveling off effect is much more pronounced as would be

expected for the heavier members of the methyl halide series[14]. These arguments also explain the relative values of the theoretical and experimental probabilities obtained for V-T/R relaxation in pure CD_3F. The theoretical CD_3F point falls on the same line with the rare gases because only its mass and thus its translational velocity are taken into account. The experimental value, however, is greater than that of a rare gas of similar mass because of the multiplicity of rotational deactivation channels available in CD_3F as opposed to the rare gas atoms. The foregoing discussion of the deactivation results in terms of the cited V-T and V-R theories is highly qualitative and intended only to explain general trends. Due to the necessarily approximate nature of such theories for complex polyatomic molecules, quantitative comparisons are not possible.

Conclusion

The vibrational energy transfer results obtained for CD_3F conform well to the patterns established by the results of previous studies on other members of the methyl halide and deuterated methyl halide series. The reasons for the particularly fast V-V equilibration have been discussed. The much slower V-T/R relaxation is consistent with a molecule where at least 903 cm^{-1} of vibrational energy (the height of the lowest fundamental) must be transferred into translation and rotation. The comparisons made with V-T/R theory are clearly qualitative, but are reasonable in terms of the trends and general rules which can be discerned among similar molecules.

Chapter 3 - CD_3Cl Studies

Experimental

The basic experiment consists of monitoring the IR fluorescence from a sample of CD_3Cl following its irradiation by the P(28) vibrational rotational line of the 9.6μ band of a Q switch CO_2 laser. A liquid nitrogen cooled InSb photovoltaic detector was used to observe the signal in the 4-5μ region while a liquid helium cooled Cu:Ge photoconductive detector was used for 14μ spectral region. Further isolation and identification of the fluorescence wavelengths was achieved by the use of IR interference filters. These allowed discrimination between ν_1, ν_4 and the overtones of ν_2, ν_5, ν_6 and ν_3 as well as the separation of ν_3 from ν_6. A detailed description of the experimental apparatus was presented earlier.[1]

---

[1] See Chapter 2

Results

Upon irradiation of a sample of CD_3Cl with the P(28) vibrational-rotational line of the 9.6μ band which corresponds to a frequency of 1039 cm^{-1} (1), fluorescence was observed in two different spectral regions, 4-5μ and $>14\mu$. By examining the partial energy level diagram for CD_3Cl presented in Figure 5 and Table 3 it becomes evident that this corresponds to absorption of the ν_2, ν_5 and emission by the ν_1, ν_4 and ν_3 respectively. Two levels are given as the absorbing state due to the complete overlap of the ν_2 and ν_5 bands at the laser pump wavelength(2). The emission wavelengths were assigned on the basis of isolation using available IR interference filters.

The exponential emission signals were time analyzed for both rise and fall. The ν_3 fluorescence was found to have an activation rate constant of 52 $msec^{-1}$ $torr^{-1}$ and a deactivation rate constant that agreed within experimental error limits with the one reported below for the ν_1, ν_4 fluorescence. A plot of rate vs. CD_3Cl pressure from which the former value was calculated is shown in Figure 6. The rate constant for the rise of ν_1, ν_4 signal was

TABLE 3

Spectral data for CD_3Cl [2]

Symmetry Species	No.	Approximate Type of Mode	Absorption Frequency (cm^{-1})
a_1	ν_1	CD_3 s-stretch	2160
a_1	ν_2	CD_3 s-deform	1029
a_1	ν_3	CCl stretch	701
e	ν_4	CD_3 d-stretch	2283
e	ν_5	CD_3 d-deform	1060
e	ν_6	CD_3 rock	768

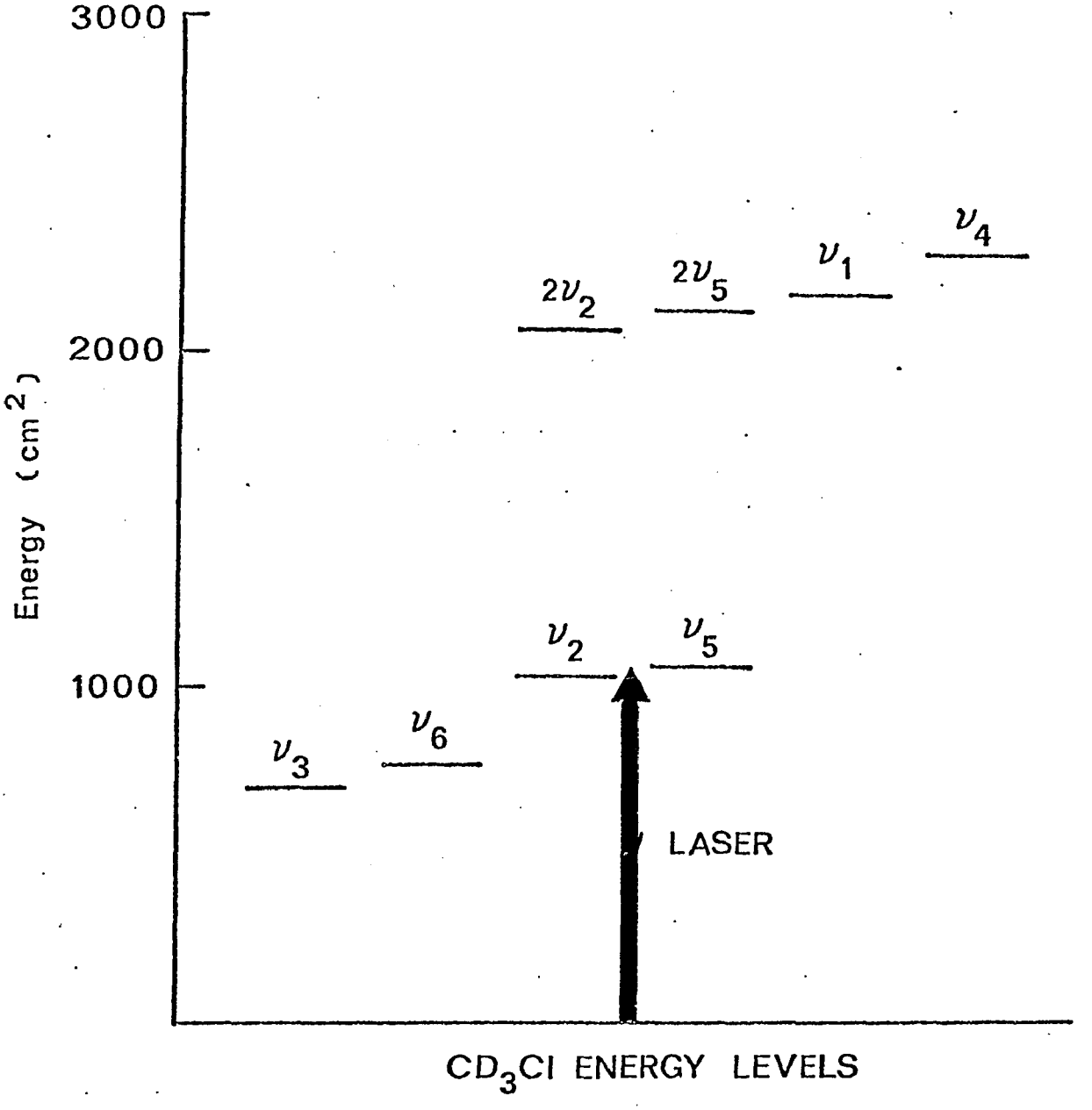

Figure 5. Partial energy level diagram for CD_3Cl

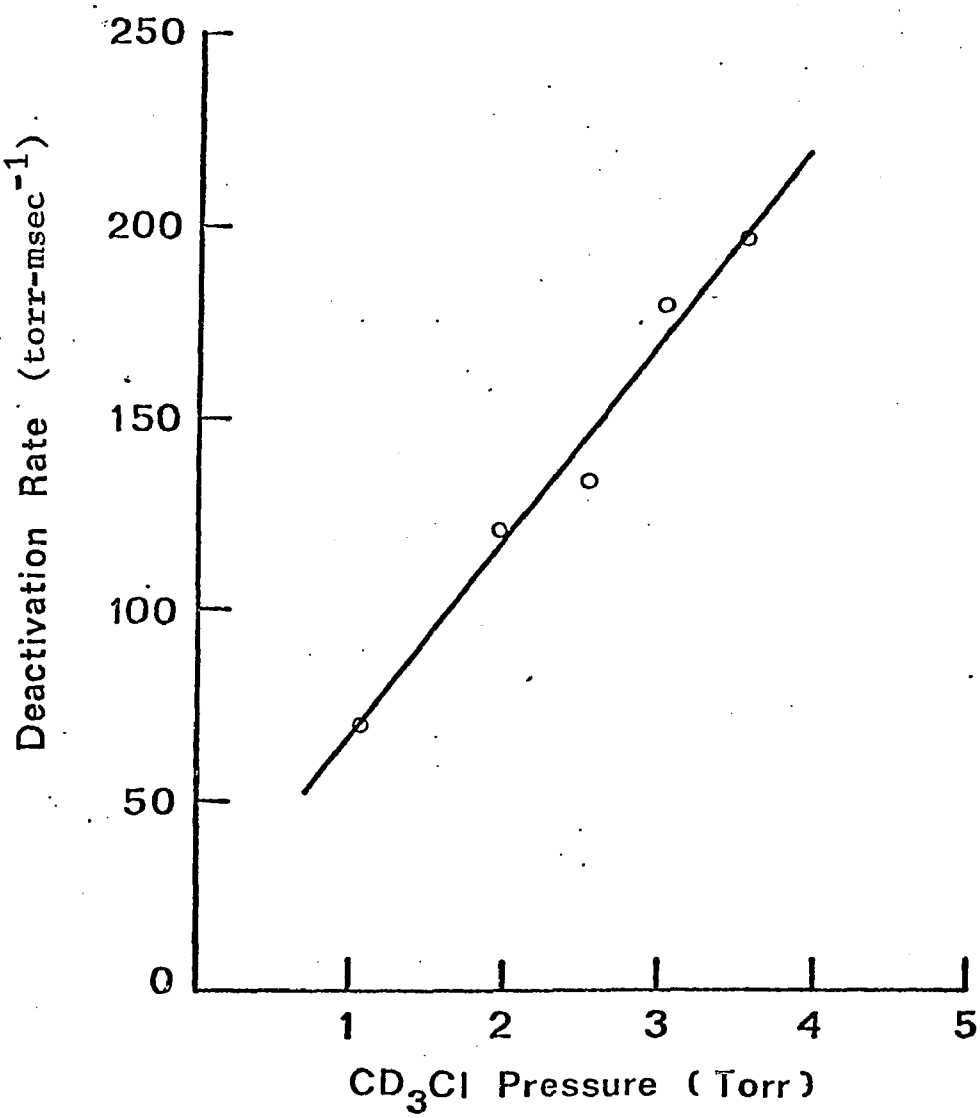

Figure 6. Plot of ν_3 fluorescence activation rate as a function of CD_3Cl pressure; slope=52 ms^{-1} $torr^{-1}$

found to be 490 $msec^{-1}$ $torr^{-1}$. However, the decay portion of this emission exhibited double exponential behavior, which resolved to yield a fast deactivation rate constant of 51 $msec^{-1}$ $torr^{-1}$ followed by a slower one of 2.8 $msec^{-1}$ $torr^{-1}$. The plot for the latter is presented in Figure 7. This slow rate was also measured as a function of rare gas pressure and is presented in Table 4 (p. 48). It should be noted that the rate obtained from the intercept of Figure 7, which corresponds to the deactivation of CD_3Cl by the given amount of Xe is consistent with the measured CD_3Cl-Xe deactivation rate constant. Analysis of the data was accomplished by semi-log plotting the fluorescence intensity vs. time to obtain deactivation rates for a set of pressures. For the ν_1, ν_4 decay this procedure resolved the double exponential curve to a fast deactivation rate prominent early in relaxation and a slower rate later in the process. Rate constants were obtained from a linear least squares treatment of the experimental rate vs. pressure curve. The reported deactivation rate constants are assigned limits of $\pm$ 10% and the activation rate constants $\pm$ 20%.

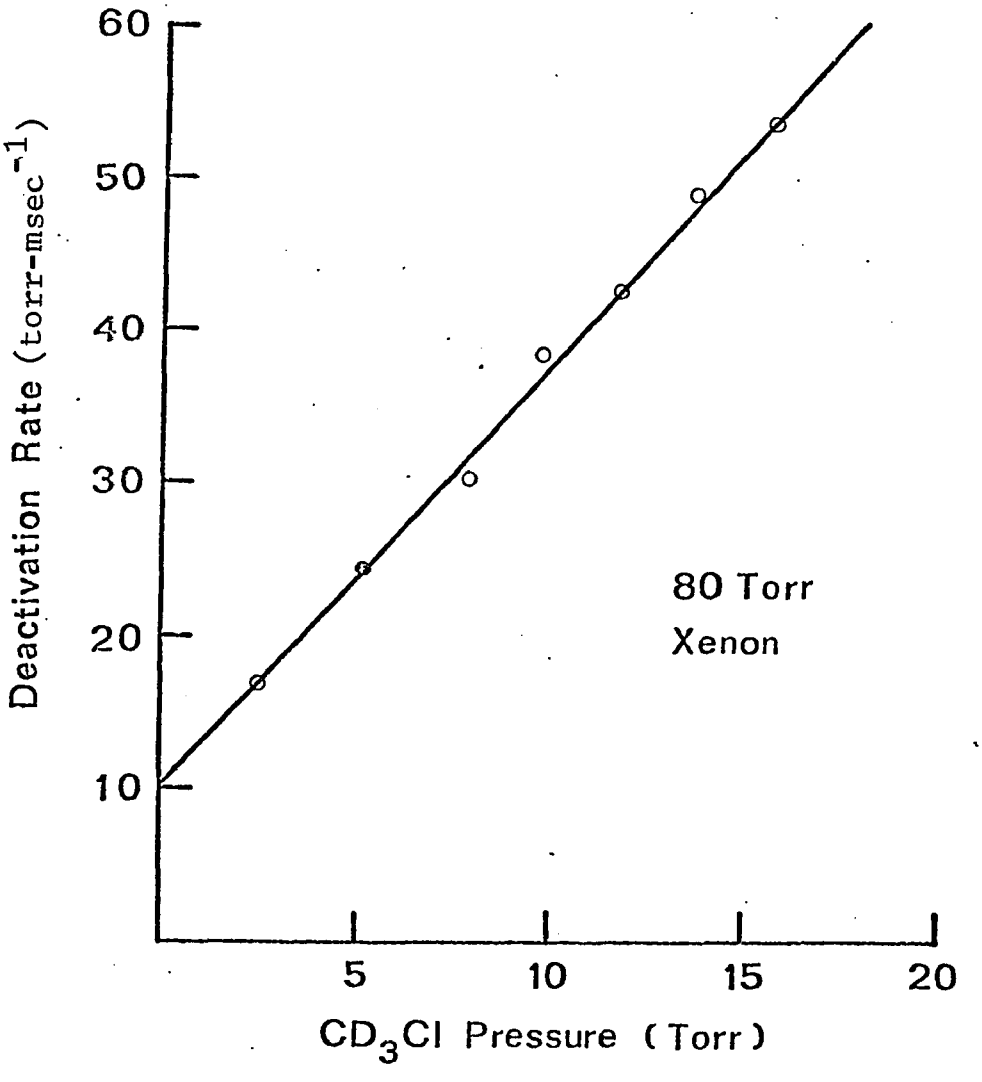

Figure 7. Plot of ν_1, ν_4 fluorescence deactivation rate as a function of CD_3Cl pressure (with a fixed Xe pressure 80 torr), slope=2.8 $ms^{-1}torr^{-1}$

The fluorescence signals observed from CD_3Cl conform to what would be expected based on the energy level distribution. After absorption of the 10μ laser radiation by the ν_2, ν_5 levels, emission is observed at lower energy from the ν_3. Signals arising from ν_2, ν_5 were not studied due to large components of scattered laser light in the 10μ region. Furthermore, fluorescence from the very weak ν_6 level was not investigated due to signal to noise limitations. Signals from overtones, i.e. $3\nu_3$, $3\nu_6$, $2\nu_2$, $2\nu_5$, did not contribute more than 10% of the total fluorescence at 4μ.

Discussion

As discussed previously[2] the rate of V-V energy transfer process is intimately related to the size of the energy defect. Processes with smaller energy defects will generally have faster rates. Based on results obtained for other molecules, the measured activation rate constant of 52 $msec^{-1}$ $torr^{-1}$ for the ν_3 fluorescence is reasonable in terms of the intermodal processes involved. These include:

$$CD_3Cl(\nu_2) + CD_3Cl(0) \rightleftharpoons CD_3Cl(\nu_3) + CD_3Cl(0) + 328\ cm^{-1} \quad (1)$$

and

$$CD_3Cl(\nu_5) + CD_3Cl(0) \rightleftharpoons CD_3Cl(\nu_3) + CD_3Cl(0) + 359\ cm^{-1} \quad (2)$$

The ν_2 and ν_5 levels, due to the overlap of their rotational states, are of course instantaneously equilibrated on the time scale of all the rates reported here. For the purpose of completeness, it should be noted that the ν_3 could also be filled by collision with the ν_6 which was itself filled by processes analogous to (1) and (2) above. However, as far as observable risetimes, the end result would be indistinguishable from the more direct routes

---

[2] Chapter 2

proposed. Indeed, though only the ν_3 fluorescence was actually observed, the above activation rate constant applies to the nearby ν_6 as well and actually represents the equilibration of the ν_2, ν_5 and ν_3, ν_6 manifolds.

The much faster activation rate constant of 490 $msec^{-1}$ $torr^{-1}$ measured for the ν_1, ν_4 fluorescence becomes understandable in terms of such processes as

$$CD_3Cl(\nu_5) + CD_3Cl(\nu_5) \rightleftharpoons CD_3Cl(\nu_1) + CD_3Cl(0) \quad -40\ cm^{-1} \tag{3}$$

$$CD_3Cl(\nu_2) + CD_3Cl(\nu_2) \rightleftharpoons CD_3Cl(\nu_1) + CD_3Cl(0) \quad -102\ cm^{-1} \tag{4}$$

and

$$CD_3Cl(\nu_2) + CD_3Cl(\nu_5) \rightleftharpoons CD_3Cl(\nu_1) + CD_3Cl(0) \quad -71\ cm^{-1} \tag{5}$$

Although these are also intermodal transfers, they are much closer to resonance. Therefore, these transfers have a much faster rate. Alternately, a pumping scheme for the ν_1 level may be proposed based on the instantaneous equilibration of the excited fundamentals and their overtones i.e. an intramodal process

$$CD_3Cl(\nu_i) + CD_3Cl(\nu_i) \rightleftharpoons CD_3Cl(2\nu_i) + CD_3Cl(0) \quad +\Delta E \qquad \Delta E \approx 0\ cm^{-1} \tag{6}$$

where i = 2, 5, followed by transfer to the fluorescing state

$$CD_3Cl(2\nu_5) + CD_3Cl(0) \rightleftharpoons CD_3Cl(\nu_1) + CD_3Cl(0) + \Delta E \qquad \Delta E \approx 40\ cm^{-1} \quad (7)$$

$$CD_3Cl(2\nu_2) + CD_3Cl(0) \rightleftharpoons CD_3Cl(\nu_1) + CD_3Cl(0) + \Delta E \qquad \Delta E \approx 102\ cm^{-1} \quad (8)$$

Mechanisms (3), (4) and (5) or (6), (7) and (8) would yield similar results.

Equations (3), (4), (5), (6), (7) and (8) take into account the collisional pumping of only the ν_1 level. Although the 4-5μ fluorescence has been assigned to both the ν_1 and ν_4 states it is believed that due to its relative band intensity, the ν_1 contributes the major share of the observed signal, and thus figures more prominently in the analysis. However, the ν_1 and ν_4 (being only 123 cm^{-1} apart in energy) equilibrate rapidly on the time scale of the ν_3, ν_6 activation.

Thus, the overall activation scheme for CD_3Cl is characterized by an instantaneous equilibration of the pumped ν_2 and ν_5 levels followed by a rapid equilibration of the ν_2, ν_5 and ν_1, ν_4 manifolds and a slower transfer to the ν_3, ν_6 levels.

This results in a quasi Boltzman equilibrium

at a higher than ambient temperature. In order for the excited system to return to equilibrium, the V-V equilibration must be followed by V-T/R and heat transfer processes.

The V-T/R rate constant for CD_3Cl self deactivation was obtained from the decay of the ν_1, ν_4 fluorescence and was observed to be 2.8 $msec^{-1}$ $torr^{-1}$. As mentioned earlier, the same value, within experimental limits of error, was obtained for the decay of the ν_3 emission. A single V-T/R relaxation rate for the entire system is a phenomenon which has been observed for the majority of molecules studied by laser induced fluorescence.[3-9] The excited vibrational levels, which are equilibrated by the faster V-V transfer, all relax simultaneously through the lowest fundamental. This level requires the least amount of energy to be given up to the translation and rotation which control the V-T/R relaxation. In the case of CD_3Cl the relevant processes are

$$CD_3Cl(\nu_3) + CD_3Cl(0) \rightleftharpoons CD_3Cl(0) + CD_3Cl(0) + 701\ cm^{-1} \quad (9)$$

and

$$CD_3Cl(\nu_6) + CD_3Cl(0) \rightleftharpoons CD_3Cl(0) + CD_3Cl(0) + 768\ cm^{-1} \quad (10)$$

The ν_6 is also included as a channel for the dumping of the excess vibrational energy because of its proximity to the lower ν_3 and because it has a larger breathing sphere parameter ($\langle A_3^2 \rangle = 0.027$, $\langle A_6^2 \rangle = 0.22$). This results in comparable theoretical probabilities of deactivation for equations (9) and (10) and will be further discussed below.

As noted, prior to and during the V-T/R relaxation, equilibrium is maintained among all the excited vibrational states by processes such as (1) - (8) and processes (11) - (14):

$$CD_3Cl(\nu_1) + CD_3Cl(0) \rightleftharpoons CD_3Cl(3\nu_6) + CD_3Cl(0) - 144\ cm^{-1} \quad (11)$$

$$CD_3Cl(\nu_1) + CD_3Cl(0) \rightleftharpoons CD_3Cl(3\nu_3) + CD_3Cl(0) + 57\ cm^{-1} \quad (12)$$

$$CD_3Cl(\nu_4) + CD_3Cl(0) \rightleftharpoons CD_3Cl(3\nu_6) + CD_3Cl(0) - 21\ cm^{-1} \quad (13)$$

$$CD_3Cl(\nu_4) + CD_3Cl(0) \rightleftharpoons CD_3Cl(3\nu_4) + CD_3Cl(0) + 180\ cm^{-1} \quad (14)$$

The second overtones of the ν_3 and ν_6 then equilibrates with their fundamentals by near resonant processes. In keeping with the earlier discussion of energy transfer, these intramodal collisional

processes are highly probable and essentially instantaneous compared to the other less resonant transfers taking place.

With a picture of a V-V equilibrated system now relaxing as a unit to the ground state, it can be seen that the fast part of the double exponential ν_1, ν_4 decay corresponds to the activation of the ν_3, ν_6 levels. The filling of the ν_3, ν_6 levels from the pumped ν_2, ν_5 states appears as a depletion or decay of the ν_1, ν_4 emission. This occurs because these latter levels are already in equilibrium with the ν_2, ν_5 due to the much faster V-V rate associated with that transfer. Indeed, the ν_3, ν_6 activation rate constant of 52 $msec^{-1}$ $torr^{-1}$ is the same (within the assigned error limits) as the constant for the fast decay of 51 $msec^{-1}$ $torr^{-1}$ measured for the first part of the ν_1, ν_4 double exponential.

A more informative way of interpreting V-T/R rate constants is to convert them into probabilities of deactivation and then compare them to results obtained from theoretical V-T/R models. This is particularly true regarding information which can be extracted from the rare gas deactivation

rates. This has been done for the data presented in Table 4 which includes CD_3Cl. In Figure 8, the probabilities are plotted against $\mu^{\frac{1}{2}}$ (the square root of the reduced mass of the collision pair). The straight lines represent theoretical probability of deactivation calculated using SSH type V-T theory (10-12) and including breathing sphere factors as modified by Stretton.(13) Relaxation through ν_3 and ν_6 is presented since the slightly higher energy of the ν_6 is offset by its larger breathing sphere parameter.

As would be expected from a model which considers the transfer of vibrational energy only to translation, the theoretical probability decreases linearly with increasing $\mu^{\frac{1}{2}}$. The experimental probability of deactivation, which is the ratio of the observed rate constant to the gas kinetic, is also presented in Figure 8. It does show linear behavior for the lighter faster moving rare gases but levels off at Kr and Xe. This leveling off is consistent with a V-R deactivation mechanism (14) and has been generally observed in other systems when the rotational velocity of the collision pair is greater than translational velocity. When this

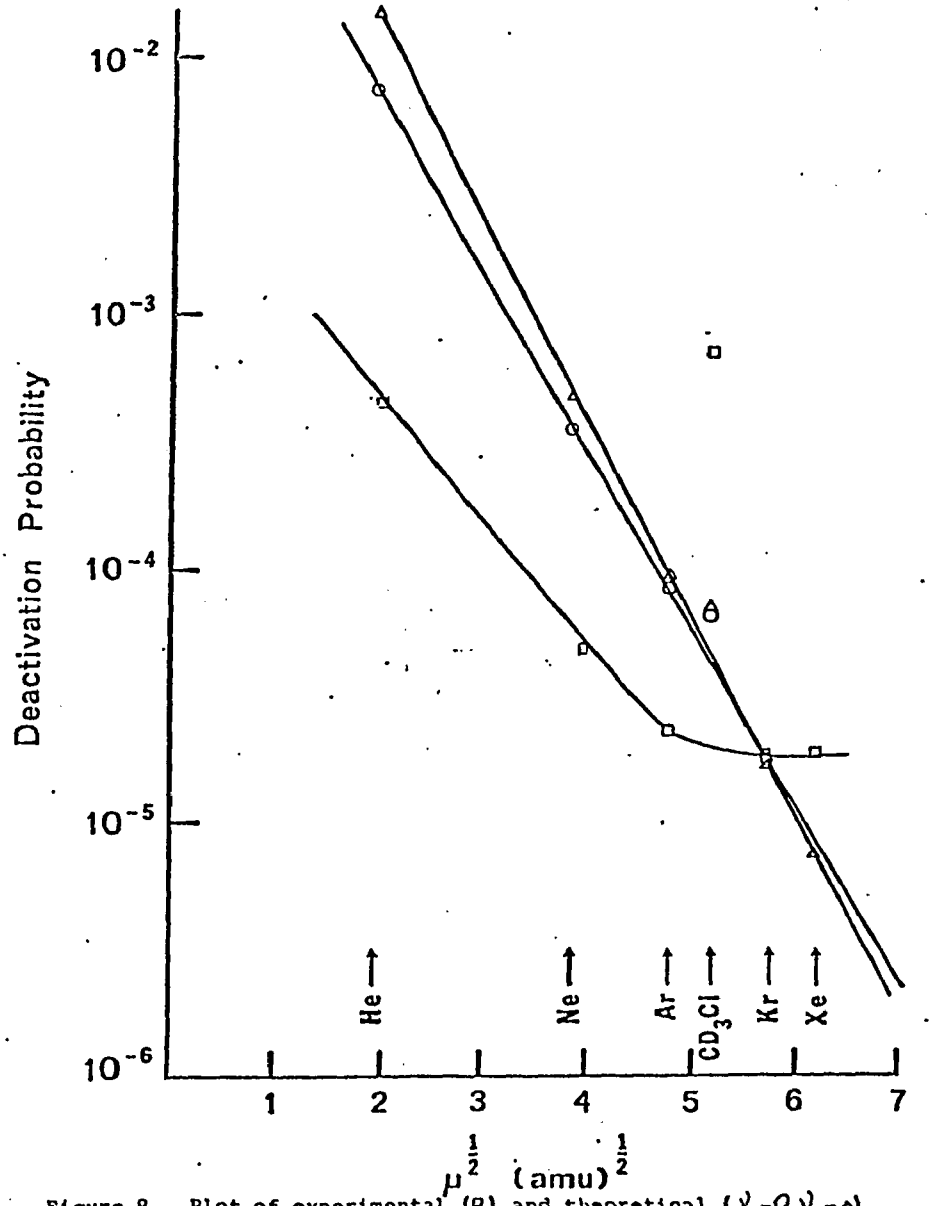

Figure 8. Plot of experimental (□) and theoretical (ν_3-O, ν_6-Δ) probabilities of deactivation as a function of the square root of the reduced mass of the collision partners

TABLE 4

DEACTIVATION RATE CONSTANTS AND PROBABILITIES

Collision Partner	$\mu^{\frac{1}{2}}_{CD_3Cl-X}$ $(amu)^{\frac{1}{2}}$	(a) σ(Å)	(b) Rate constant $(msec^{-1}torr^{-1})$	(c) Z	(d) $P_{exp.}$ x 10^3	(e) $P_{theor.}$ ν_3 x 10^3	(e) $P_{theor.}$ ν_6 x 10^3
CD_3Cl	5.17	4.04	2.8	2900	0.346	0.0652	0.0694
He	1.93	2.58	7.3	2000	0.502	7.47	14.8
Ne	3.83	2.86	0.48	16600	0.0603	0.347	0.468
Ar	4.78	3.47	0.17	44400	0.0225	0.0825	0.0937
Kr	5.71	3.61	0.12	54700	0.0183	0.0174	0.0169
Xe	6.16	4.06	0.13	52400	0.0191	0.00825	0.00747

(a) J. O. Hirschfelder, C. F. Curtis and R. B. Bird, Molecular Theory of Gases and Liquids (Wiley, New York, 1954).

(b) Error limits are $\pm$ 10% of reported values.

(c) Number of collisions needed for deactivation, rounded off to nearest hundreds place

$$Z = 2.56 \times 10^6 \left(\frac{\sigma_a + \sigma_b}{2}\right)^2 \mu^{-\frac{1}{2}} \ (10^{-3}/\text{rate constant})$$

(d) Experimental probability/collision $P_{exp.} = 1/Z$

(e) Theoretical probability of deactivation through ν_3 and ν_6, calculated using SSH theory and including breathing sphere parameters $\langle A_3^2 \rangle = 0.0333$ and $\langle A_6^2 \rangle = 0.1011$.

is the case, V-R processes become more important than V-T processes. Thus, when V-R predominates (as for the heavier rare gases) similar probabilities are obtained since these atoms do not supply any rotational deactivation channels to the system. The importance of the availability of additional channels is illustrated by the more than one order of magnitude difference between the experimental probability for CD_3Cl self relaxation and the expected probability according to the experimental curve for a rare gas of similar mass.

It should be noted that the above discussion of the deactivation results in terms of V-T and V-R theories is qualitative at best. The present state of such theories precludes exact quantitative comparisons, yet general trends can be deduced.

Subsequent to the V-V and V-T/R processes a new Boltzman equilibrium is established. The final step in the complete relaxation of the laser excited gas sample is the return of the translationally hot gas to ambient temperature through heat and mass transport to the cell walls.

A comparison of the V-T/R deactivation results obtained for CD_3Cl with those of CH_3Cl serves to

further illustrate some of the points discussed above. The CH_3Cl self deactivation rate constant was found to be 7.5 $msec^{-1}$ $torr^{-1}$ while the rare gases yielded 3.1, 0.51, 0.54, and 0.53 $msec^{-1}$ $torr^{-1}$ for He, Ne, Ar, Kr, and Xe respectively.[5] For all these species, except He, the rate constants are larger than the corresponding values in CD_3Cl. This is due to the fact that the greater rotational velocity of the hydrogen compound increases the probability per collision of V-R relaxation. The availability of the additional rotationl deactivation channels results in a faster rate. The increased importance of V-R processes in CH_3Cl as compared to CD_3Cl is also evident from the observation that in going from He to Xe the deactivation rate constants level off earlier for the former compound than for the latter. Another factor contributing to the larger rate constants for CH_3Cl is the magnitude of the ν_6 breathing sphere parameter which is twice as great in CH_3Cl as it is in CD_3Cl.

Conclusion

The results obtained for V-V energy transfer rates of CD_3Cl are in good qualitative agreement with results obtained for the non-deuterated species and theoretical aspects of energy transfer. As expected, a fast V-V equilibration of all excited vibrational levels is followed by a single slower rate for relaxation of the entire system to the ground state. Furthermore, the importance of V-R processes can be seen in the form of a leveling off of deactivation probability as the collision partner is changed to heavier rare gases.

Appendix

SSH Calculations

The total energy of a gas may be expressed as the sum of the energies of translation, rotation, vibration, etc.

$$E = E_{trans}\ (T) + E_{rot}\ (T_r) + E_{vib}\ (T_v) + \ldots \quad (1)$$

where T, T_r, T_v are "temperatures", but are not necessarily equal to one another.

In 1936, Bethe & Teller[1,2] described the lack of adjustment of the vibrational degrees of freedom for a pure diatomic gas:

$$\frac{dE_{vib}\ (T_v)}{dt} = \frac{1}{\tau}\ \{E_{vib}\ (T) - E_{vib}\ (T_v)\} \quad (2)$$

Where T is the temperature of the translational degrees of freedom, T_v is the temperature of the vibrational degrees of freedom and τ is called the relaxation time of the gas.

Assuming that energy transfer between degrees of freedom can occur only during a molecular collision, the rate of energy transfer must be inversely proportional to the number of collisions a molecule experiences per second, M_{aa}. Since not every collision is effective in transferring energy, the relaxation time must also be inversely proportional to the probability of such an energy exchange,

denoted by P. Thus for the relaxation time, we may write

$$\tau = \frac{1}{M_{aa} P} \qquad (3)$$

For a gas composed of polyatomic molecules or mixtures of different types of molecules, there arises the possibility of energy exchange between the different vibrational degrees of freedom during a collision as well as exchanges with the translational degrees of freedom. A separate relaxation time must be ascribed to each of these energy transfers. To describe the gas system, one requires additional equations more complicated than eq (2). In the theory, developed by Schwartz, Slawsky, and Herzfeld (SSH) [3] for diatomic gases and modified by Tanczos[4] for polyatomic gases undergoing a simultaneous change of a vibrational state in each of the colliding molecules, one considers only the short range part of the intermolecular collision potential, and ignores molecular rotations, while attempting to make ab initio calculations of transition probabilities. The probability of a simultaneous vibrational transition due to a molecular collision is given by[5]:

$$P_{k\to l}^{i\to j}(a,b) = P_0(a)P_0(b)\{V(k-j)\}^2\{V(k-l)\}^2\, 8\left(\frac{\mu}{2kT}\right)$$

$$\times \exp -(\Phi o/kT)\left[\frac{8\pi\mu\Delta E}{h^2}\right]^2 \int_o^\infty f(u)\,du$$

$$f(u) = \frac{u}{\alpha^4}\left[\frac{r_c}{r_0}\right]^2 \exp\left[\frac{-\mu u^2}{2kT}\right]\left[\frac{\exp(L-L')}{1-\exp(L-L')^2}\right]$$

$$L = \frac{4\pi^2\mu u}{\alpha h}$$

$$L' = \frac{4\pi^2\mu v}{\alpha h} \qquad (4)$$

in which

$P_0(a)$, $P_0(b)$ - steric factors for molecules a and b

$V(i-j)$, $V(k-l)$ - matrix elements of the perturbation potential

μ - reduced mass of the collision pair

Φ_o - minimum of intermolecular potential, and equal to $-(\varepsilon_a\varepsilon_b)^{\frac{1}{2}}$, where ε is the Lennard-Jones well depth

ΔE - the amount of vibrational energy converted into translational energy

u - initial relative velocity

v - final relative velocity,

$$v = u\left(1 + \frac{2\Delta E}{\mu u^2}\right)^{\frac{1}{2}}$$

α - intermolecular repulsion parameter

$\frac{r_c}{r_0}$ - the ratio of the distance of closest approach to the gas kinetic diameter. For thermal velocity collisions this number is 1.

This equation may be considered to have three parts represented by[6]:

$$P_{i-f} = g_f P_0 |u_{i-f}| I(\Delta E, T, \mu, \alpha, \varepsilon) \quad (5)$$

First we include a geometrical or steric factor, P_0, followed by a translational factor, I, containing the effects of the relative velocity and energy deficit on the translation probability. Finally, a vibrational factor specified by the matrix elements of the interaction potential accounts for the probability of a vibrational transition. These matrix elements have been worked out for various vibrational transitions[5] and are listed in Table 5. The entire probability is multiplied by a constant, g_f, the degeneracy of the final state.

In order to account for the various amplitudes of the simultaneous occurring vibrations, a factor known as the breathing sphere parameter[5] is intro-

TABLE 5

HARMONIC OSCILLATOR VIBRATIONAL FACTORS

Transition	Vibrational Factor[a,b]
$\nu_i \rightarrow 0$	$\alpha^2(\bar{A}_i^2)/2\gamma \equiv V_i$
$2\nu_i \rightarrow 0$	$\alpha^4(\bar{A}_i^2)/8\gamma^2 = V^2{}_i/2$
$3\nu_i \rightarrow 0$	$(V_i)^3/3$
$n\nu_i \rightarrow 0$	$(V_i)^n/n!$
$(\nu_i+\nu_j) \rightarrow 0$	$\alpha^2(\bar{A}_i^2)/2\gamma_i \cdot \alpha^2(A_j^2)/2\gamma j = V_i V_j$
$(2\nu_i+\nu_j) \rightarrow 0$	$(V_i)^2 \cdot V_j/2$
$(3\nu_i+\nu_j) \rightarrow 0$	$(V_i)^3 \cdot V_j/3$
$(n\nu_i+\nu_j) \rightarrow 0$	$(V_i)^n \cdot V_j/n!$

(a) Reference (7)

(b) Reference (5)

(c) $\gamma = 4\pi^2\nu/h$

duced into the vibrational matrix elements. The breathing sphere parameter, $\langle A_i \rangle$, is defined as the average Cartesian displacement of the surface atoms of the molecule for a unit change in a given normal coordinate. Thus in this model each molecule is represented as a sphere whose surface is in motion with the frequency and amplitude of the vibrational mode.

SSH calculations do not allow for vibrational transitions explicitly due to long range forces (dipole-dipole, dipole-quadrupole) yet obtain good results for molecules in which relatively large amounts of energy goes into translations.

References

Chapter 1

References

1. P. Borrell, Adv. Mole, Relax. Proc. 1, 69 (1967-68).

2. S. M. Lee and A. M. Ronn, Chem. Phys. Lett. 26, 497 (1974).

3. L. A. Gamss, A. M. Ronn and G. W. Flynn, Bull. Am. Phys. Soc. 20, 684 (1975).

4. L. A. Gamss, B. H. Kohn, M. I. Pollack and A. M. Ronn, Bull. Am. Phys. Soc. 21, 14 (1976).

5. L. A. Gamss, B. H. Kohn, A. M. Ronn, and G. W. Flynn, Chem. Phys. Lett. 41, 413 (1976).

6. L. A. Gamss, B. H. Kohn, M. I. Pollack and A. M. Ronn, Chem. Phys. 18, 85 (1976).

Chapter 2

References

1. K. M. Baird, H. D. Riccius, and K. J. Siemsen, Optics Communications, 6, 91 (1972).

2. T. Shimanouchi, "Tables of Molecular Vibrational Frequencies," (NSRDS NBS 39).

3. G. W. Flynn, in Chemical and biochemical application of lasers, ed. C. B. Moore (Academic Press, New York, 1974).

4. L. A. Gamss and A. M. Ronn, Chem. Phys., 9, 319 (1975).

5. B. L. Earl, P. C. Isolani and A. M. Ronn, Chem. Phys. Lett., 39, 95 (1976).

6. Z. Karny, A. M. Ronn, E. Weitz, and G. W. Flynn, Chem. Phys. Lett., 17, 347 (1972).

7. R. N. Schwartz, Z. I. Slawsky and K. F. Herzfeld, J. Chem. Phys., 20, 1591 (1952).

8. R. N. Schwartz and K. F. Herzfeld, J. Chem. Phys., 22, 767 (1954).

9. J. L. Stretton, TRANS. FARADAY SOC., 61, 1053 (1965).

10. F. R. Tanczos, J. Chem. Phys., 25, 439 (1965).

11. E. W. Jones, R. J. L. Popplewell and H. W. Thomson, Proc. Roy. Soc., A290, 490 (1966).

12. L. A. Gamss, B. H. Kohn, M. I. Pollack, and A. M. Ronn, Chem. Phys., 18, 85 (1976).

13. S. T. Lin, B. L. Earl and A. M. Ronn, Chem. Phys., 16, 117 (1976).

14. Y. Langsam, S. M. Lee, and A. M. Ronn, Chem. Phys., 15, 43 (1976).

15. E. Weitz, G. W. Flynn, J. Chem. Phys., 58, 2781 (1973).

16. F. R. Grabiner and G. W. Flynn, J. Chem. Phys., 60, 398 (1974).

17. B. L. Earl and A. M. Ronn, Chem. Phys., 12, 113 (1976).

18. Y. Langsam, S. M. Lee and A. M. Ronn, Chem. Phys., 14, 375 (1976).

19. E. Weitz and G. W. Flynn, J. Chem. Phys., 56, 6060 (1972).

20. E. Weitz and G. W. Flynn, J. Chem. Phys., 58, 2679 (1973).

21. C. B. Moore, J. Chem. Phys., 43, 2979 (1965).

Chapter 3

References

1. K. M. Baird, H. D. Riccius and K. J. Siemsen, Optics Communications, 6, 91 (1972).

2. A. D. Dickson, I. M. Mills and B. Crawford Jr., J. Chem. Phys., 29, 445 (1957).

3. E. Weitz and G. W. Flynn, J. Chem. Phys., 58, 2679 (1973).

4. E. Weitz and G. W. Flynn, J. Chem. Phys., 56, 6060 (1972).

5. J. T. Knudtson and G. W. Flynn, J. Chem. Phys., 58, 2684 (1973).

6. B. L. Earl and A. M. Ronn, Chem. Phys., 12, 113 (1976).

7. S. T. Lin, B. L. Earl and A. M. Ronn, Chem. Phys., 16, 117 (1976).

8. Y. Langsam, S. M. Lee and A. M. Ronn, Chem. Phys., 14, 375 (1976).

9. Y. Langsam, S. M. Lee and A. M. Ronn, Chem. Phys., 15, 43 (1976).

10. R. N. Schwartz, Z. I. Slawsky and K. F. Herzfeld, J. Chem. Phys., 20, 1591 (1952).

11. R. N. Schwartz and K. F. Herzfeld, J. Chem. Phys., 22, 767 (1954).

12. F. R. Tanczos, J. Chem. Phys., 25, 439 (1965).

13. J. L. Stretton, TRANS. FARADAY SOC., 61, 1053 (1965).

14. O. B. Moore, J. Chem. Phys., 43, 2979 (1965).

Appendix

References

1. L. Landau and E. Teller, Phys. Z, d. Sowjetunion, 10, 34 (1936).

2. H. A. Bethe and E. Teller, Aberdeen Proving Ground Report X-117.

3. R. N. Schwartz, A. I. Slawsky, K. T. Herzfeld, J. Chem. Phys., 20, 1591 (1952).

4. F. R. Tanczos, J. Chem. Phys., 25, 439 (1956).

5. J. L. Stretton, TRANS. FARADAY SOC., 61, 1053 (1965).

6. J. T. Yardley and C. B. Moore, J. Chem. Phys., 49, 11, 1111 (1968).

7. E. B. Wilson, J. C. Decius and P. C. Cross, "Molecular Vibrations", (McGraw-Hill, New York, 1955).